

Double-Shell Tank Integrity Project High Level Waste Chemistry Optimization

Prepared for the U.S. Department of Energy
Assistant Secretary for Environmental Management

Contractor for the U.S. Department of Energy
Office of River Protection under Contract DE-AC27-99RL14047

CH2MHILL
Hanford Group, Inc.

*P.O. Box 1500
Richland, Washington*

**Approved for Public Release:
Further Dissemination Unlimited**

Double-Shell Tank Integrity Project High Level Waste Chemistry Optimization

Chung-King Liu
Department of Energy - Office of River Protection

C. S. Brossia, Ph.D.
CC Technologies, Inc.

D. J. Washenfelder
H. S. Berman
K. D. Boomer
CH2M HILL Hanford Group, Inc.

Date Published
January 2008

To Be Presented at
WM 2008 Conference

Waste Management Symposia, Inc.
Phoenix, Arizona

February 24-28, 2008

Published in
Proceedings of 2008 Waste Management Conference

Prepared for the U.S. Department of Energy
Assistant Secretary for Environmental Management

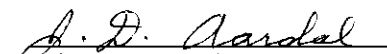
Contractor for the U.S. Department of Energy
Office of River Protection under Contract DE-AC27-99RL14047

CH2MHILL
Hanford Group, Inc.

P. O. Box 1500
Richland, Washington

Copyright License

By acceptance of this article, the publisher and/or recipient acknowledges the U.S. Government's right to retain a nonexclusive, royalty-free license in and to any copyright covering this paper.


Release Approval 01/27/2008
Date

Approved for Public Release:
Further Dissemination Unlimited

LEGAL DISCLAIMER

This report was prepared as an account of work sponsored by an agency of the United States Government. Neither the United States Government nor any agency thereof, nor any of their employees, nor any of their contractors, subcontractors or their employees, makes any warranty, express or implied, or assumes any legal liability or responsibility for the accuracy, completeness, or any third party's use or the results of such use of any information, apparatus, product, or process disclosed, or represents that its use would not infringe privately owned rights. Reference herein to any specific commercial product, process, or service by trade name, trademark, manufacturer, or otherwise, does not necessarily constitute or imply its endorsement, recommendation, or favoring by the United States Government or any agency thereof or its contractors or subcontractors. The views and opinions of authors expressed herein do not necessarily state or reflect those of the United States Government or any agency thereof.

This report has been reproduced from the best available copy.
Available in paper copy.

**Double-Shell Tank Integrity Project
High Level Waste Chemistry Optimization - 8181**

Chung King Liu

U.S. Department of Energy, Office of River Protection
P.O. Box 450, Richland Richland, Washington 99352

D.J. Washenfelder, H.S. Berman, and K.D. Boomer
CH2M HILL Hanford Group, Inc.
P.O. Box 1500, Richland, Washington 99352

C.S. Brossia, Ph.D.
CC Technologies, Inc.
5777 Frantz Road, Dublin, Ohio 43017

ABSTRACT

The U.S. Department of Energy's Office (DOE) of River Protection (ORP) has a continuing program for chemical optimization to better characterize corrosion behavior of High-Level Waste (HLW). The DOE controls the chemistry in its HLW to minimize the propensity of localized corrosion, such as pitting, and stress corrosion cracking (SCC) in nitrate-containing solutions. By improving the control of localized corrosion and SCC, the ORP can increase the life of the Double-Shell Tank (DST) carbon steel structural components and reduce overall mission costs. The carbon steel tanks at the Hanford Site are critical to the mission of safely managing stored HLW until it can be treated for disposal.

The DOE has historically used additions of sodium hydroxide to retard corrosion processes in HLW tanks. This also increases the amount of waste to be treated. The reactions with carbon dioxide from the air and solid chemical species in the tank continually deplete the hydroxide ion concentration, which then requires continued additions. The DOE can reduce overall costs for caustic addition and treatment of waste, and more effectively utilize waste storage capacity by minimizing these chemical additions.

Hydroxide addition is a means to control localized and stress corrosion cracking in carbon steel by providing a passive environment. The exact mechanism that causes nitrate to drive the corrosion process is not yet clear. The SCC is less of a concern in the newer stress relieved double shell tanks due to reduced residual stress. The optimization of waste chemistry will further reduce the propensity for SCC.

The corrosion testing performed to optimize waste chemistry included cyclic potentiodynamic polarization studies, slow strain rate tests, and stress intensity factor/crack growth rate determinations. Laboratory experimental evidence suggests that nitrite is a highly effective inhibitor for pitting and SCC in alkaline nitrate environments. Revision of the corrosion control strategies to a nitrite-based control, where there is no constant depletion mechanism as with hydroxide, should greatly enhance tank lifetime, tank space availability, and reduce downstream reprocessing costs by reducing chemical addition to the tanks.

INTRODUCTION

The U.S. Department of Energy River Protection Project (RPP) stores radioactive waste from past fuel reprocessing at the Hanford Site. Beginning in 1968 the United States Atomic Energy Commission (AEC) began the construction of Double-Shell Tanks (DSTs) to augment 149 Single-Shell Tanks (SSTs) at the site. These tanks were specified to have 20 to 50 year design lives, which included a general corrosion allowance of 0.001 inch per year. The AEC incorporated design measures to reduce the likelihood of Stress Corrosion Cracking (SCC). Chemistry controls were invoked to prevent this phenomenon from occurring.

Chemical additions to maintain waste within specifications consumes space in the DST system and increases the volume of waste to be processed through treatment facilities. The increased volume leads to a longer processing duration and increases the cost to perform the RPP mission.

Recent advances in the understanding of the waste storage conditions are eliminating chemical additions and increasing the tank operating life span. This advanced understanding has confirmed underlying basis of the Ultrasonic Testing (UT) program. These two program elements along with the visual inspection program provide a strong technical basis to the DST Integrity Project.

BACKGROUND

Current waste chemistry limits for corrosion control in DSTs are summarized in Table I. These limits reduce the potential for general corrosion, pit corrosion, and Stress Corrosion Cracking (SCC). The limits are based on maintaining the ratio of the concentration of corrosion inhibitors (hydroxide and nitrite ions) to the concentration of nitrate ions for two nitrate ion concentration levels ($[\text{NO}_3^-] \leq 1.0\text{M}$ and $1.0\text{M} < [\text{NO}_3^-] \leq 3.0\text{M}$) and maintaining the inhibitor concentration greater than or equal to 1.2M at $[\text{NO}_3^-] \geq 3.0\text{M}$. In addition to the ratios, the limits specify the minimum concentrations for hydroxide and nitrite ions. Operational considerations and hydroxide depletion lead to chemical additions in excess of these limits to maintain these requirements throughout the tank waste for up to five years after the additions.

Table I. Current Hanford Double-Shell Tank Waste Chemistry Limits

[NO ₃ ⁻] Range	Parameter	Waste Temperature Range (°F)		
		T < 167	167 ≤ T ≤ 212	T > 212
[NO ₃ ⁻] ≤ 1.0M	[OH ⁻]	$0.01\text{M} \leq [\text{OH}^-] \leq 8\text{M}$	$0.01\text{M} \leq [\text{OH}^-] \leq 5\text{M}$	$0.01\text{M} \leq [\text{OH}^-] \leq 4\text{M}$
	[NO ₂ ⁻]	$0.011\text{M} \leq [\text{NO}_2^-] \leq 5.5\text{M}$		
	$[\text{NO}_3^-]/([\text{NO}_2^-] + [\text{OH}^-])$	< 2.5		
$1.0\text{M} < [\text{NO}_3^-] \leq 3.0\text{M}$	[OH ⁻]	$0.01([\text{NO}_3^-]) \leq [\text{OH}^-] \leq 10\text{M}$		$0.01([\text{NO}_3^-]) \leq [\text{OH}^-] \leq 4\text{M}$
	[OH ⁻] + [NO ₂ ⁻]	$\geq 0.4([\text{NO}_3^-])$		
[NO ₃ ⁻] ≥ 3.0M	[OH ⁻]	$0.3\text{M} \leq [\text{OH}^-] \leq 10\text{M}$		$0.3\text{M} \leq [\text{OH}^-] \leq 4\text{M}$
	[OH ⁻] + [NO ₂ ⁻]	$\geq 1.2\text{M}$		
	[NO ₃ ⁻]	$\leq 5.5\text{M}$		

The basis for waste chemistry limits in DST comes from data developed at Hanford and the Savannah River Site (SRS). The majority of the requirements come from work done by Ondrejcin (DP-1478, *Prediction of Stress Corrosion of Carbon Steel by Nuclear Process Liquid Waste*) in the 1970s to prevent SCC. The basis for these criteria is work that examined the waste chemistry requirements for newly generated and concentrated waste at the SRS. In setting these requirements, SRS established a single set of requirements for operational simplicity. As such they established requirements for their worst case, which was newly generated waste stored in non-Post -Weld Heat Treated (PWHT) A285 Carbon Steel exposed to temperature up to 100 °C at pH > 11. Hanford adopted these criteria in 1980.

The current storage conditions and tank construction at Hanford are more conservative than those used in the SRS worst case scenario basis for SCC prevention. The storage of the all the waste at Hanford is below 80 °C (176 °F) with vast majority of the waste stored at temperature below 40 °C (104 °F). All of the Hanford DSTs have been constructed from higher tensile strength carbon steel than A285 Carbon Steel (A515 [241-AY and 241-AZ], A516 [241-SY], and A537 [241-AN, 241-AP, and 241-AW]), which have been PWHT at 570 °C (1050 °F) ± 30 °C (50 °F). No PWHT tank has experienced SCC at SRS or Hanford since this method of construction was adopted. In addition, wall thickness was increased for later tanks, which allows the wall to better handle the stresses, lowering their susceptibility of SSC.

Maintaining these controls has led to the addition of more than 500 metric tons of sodium since 2000. At current storage conditions, these additions have consumed an equivalent volume of one DST. Planning for the retrieval waste from 241-S-112 identified the need to add 200 metric tons of sodium to retrieve the 900 metric tons in the SST. The addition was avoided by modifying the retrieval plan. The chemicals added translate to the production of more low activity waste for disposal at Hanford, which in turn increases the operational duration and cost for the mission of the RPP. As a result of the 241-S-112 impact and other similar future impacts, the RPP has looked for means to optimize the chemical control of corrosion in the DSTs.

TEST PROGRAM

To conduct the chemistry optimization program, CH2M HILL uses accelerated corrosion testing. These tests use ASTM standard procedures for Cyclic Potentiodynamic Polarization (CPP) measurements, Slow Strain Rate (SSR) testing, and crack stress intensity Factor (K_{Isc}). To date, the testing has focused on the waste in two tanks Tank 241-AN-107 (AN-107) and Tank 241-AY-102 (AY-102). For AN-107, the testing was expanded to include Tank 241-AN-102 (AN-102), which contains waste similar to the waste stored in AN-107. For AY-102, the testing accounted for waste recently transferred from Tank 241-AP-101 (AP-101). For the remainder of the paper, references made to AN-107 and AY-102 address the test program, which includes the other chemistries tested.

The waste in these tanks was selected for testing because the interstitial liquids in the solid layer of the tanks don't comply with the existing chemistry control limits. Specifically, AN-107 has been out of specification since waste was originally added to the tank. Sodium hydroxide was added to the tank in 2002, which brought the supernatant into specification. Insufficient convective mixing between the supernatant and the interstitial liquid failed to bring the lower layer of the waste into compliance. The chemistry optimization showed that expensive remediation by installation of a mixing pump was unnecessary. Mixing was not needed because of the low propensity for corrosion to occur. The chemistry control for AN-107 interstitial liquid has been changed and changes for other tanks are in progress at this time (e.g., AN-102).

Materials and Specimens

All test specimens were fabricated from vintage metals. For Tanks AN-107 and AN-102, three 3'x2'x1" as-supplied plates of ASTM A537 Class 2 carbon steel material that had been heat-treated to obtain material properties similar to those of the Class 1 carbon steel were used. For Tank AY-102, one 2'x2'x1" as-supplied plate of AAR TC 128 Grade tank car steel, which is similar to the steel used in the tank construction was used. Fig. 1 shows the microstructures of the steel tested during the course of this work. The steel used for the AN-107 work shows a normalized structure. The steel used for the AY-102 work has a banded structure that indicates that the steel has been rolled at some time during its processing.

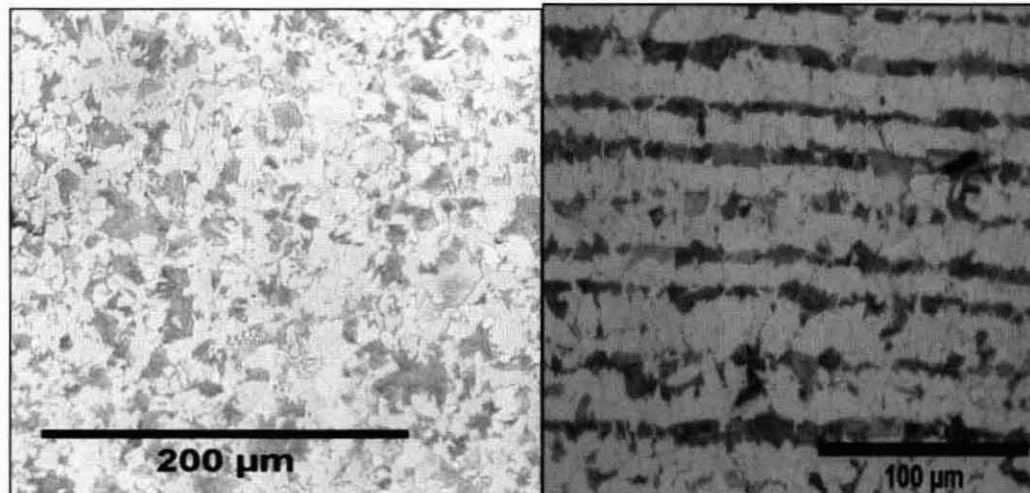


Fig. 1. Comparison of the Microstructures Materials Tested for Tanks 241-AN-107 and 241-AY-102.

Three main specimen geometries were utilized in this work: rounded 1.25 inch long by 0.188 inch diameter studs for the CPP tests, 8 inch long by 0.25 inch diameter tensile test specimens that tapered to 0.125 inch in the middle for the SSR tests, and compact tension specimens for crack growth. Specimens were fabricated by Metal Samples Company in Munford, AL or Metcut Research, Inc. in Cincinnati, OH. Material close to the flame cuts at the edges of the plates was avoided for specimen fabrication to ensure consistent microstructures. The SSR test specimens were fabricated such that the longitudinal axis was in the plate rolling direction (i.e., longitudinal orientation). Compact tension specimens were fabricated such that the pre-crack was in the plate rolling direction (i.e., transverse-longitudinal orientation).

Test Solutions

The AN-107 waste simulant represents waste similar to waste in the majority of the DSTs. These wastes are dominated by nitrate chemistry. The waste in AY-102 consists of two distinct layers. The upper portion is similar to the waste in the AN-107 simulant (AP-101 waste), but the lower portion contains waste low in nitrate and high in total inorganic carbon (TIC) or carbonate waste. As such the examination of these two waste types provides a test regime that covers essentially all of the waste in the DST system.

In developing simulants for the two test regimes, different approaches had to be taken. For AN-107, a base simulant was developed and inhibitor concentrations were adjusted over a wide range to evaluate their influence on mitigating SCC caused by nitrate. With the Tank AY-102 testing, a different approach had to be taken because of a wider range of conditions in the tank caused by the recent addition of waste from AP-101. The simulants represent these two layers and the composition of the waste once it was mixed. Table II shows the different simulants tested as part of the AY-102 corrosion work. In these simulants, the interstitial liquids are the carbonate based waste and the supernatants are the nitrate based wastes. Table III shows the range of chemical concentrations used for AN-107 and AY-102 simulants.

Table II. Tank 241-AY-102 Test Simulants

Acronym	Tank	Simulant
AP101-TSC	AP-101	Transferred Supernatant Composition
AY102-ACS	AY-102	Aged Combined Supernatant
AY102-AIL	AY-102	Aged Interstitial Liquid
AY102-ATL	AY-102	Aged Total Liquid
AY102-CSC	AY-102	Combined Supernatant Composition
AY102-PIL	AY-102	Present Interstitial Liquid

Table III. Tank Simulant Concentration Ranges

		Tank Simulant		
		241-AN-107 Interstitial Liquid*	241-AY-102 Interstitial Liquid	241-AY-102 Supernatant
Nitrate	Starting Point	3.7 <u>M</u>	0.002	1.97 <u>M</u>
	End Point	2.4 <u>M</u>	0.002	1.12 <u>M</u>
	Range Tested	1.5 – 2.7 <u>M</u>	0.002 – 1.967 <u>M</u>	0.21 – 2.13 <u>M</u>
Nitrite	Starting Point	1.2 <u>M</u>	0.001 <u>M</u>	0.94 <u>M</u>
	End Point	2.3 <u>M</u>	0.001 <u>M</u>	1.27 <u>M</u>
	Range Tested	0 -7 <u>M</u>	N/A	0 – 1.2 <u>M</u>
Hydroxide	Starting Point	pH 11	pH 11	pH 14+
	End Point	pH 10	pH 11	pH 14+
	Range Tested	pH 7 to 13.5	N/A	N/A
Total Inorganic Carbon	Starting Point	1.48 <u>M</u>	1.02 <u>M</u>	0.4 <u>M</u>
	End Point	--	0.935 <u>M</u>	1.12 <u>M</u>
	Range Tested	N/A	0.935 -1.02 <u>M</u>	0 – 1.12 <u>M</u>
Chloride	Starting Point	0.1 <u>M</u>	--	--
	End Point	0.1 <u>M</u>	--	--
	Range Tested	0.1 – 0.2 <u>M</u>	--	--

* The Tank AN-107 waste compositions bound the composition of 241-AN-102 for nitrate, nitrite, and hydroxide, and Total Organic Carbon. Testing for 241-AN-102 used this simulant and increased the chloride concentration to 0.2 M.

OPEN CIRCUIT POTENTIAL MONITORING AND CYCLIC POTENTIODYNAMIC POLARIZATION TESTING

The cyclic potentiodynamic polarization (CPP) is used to identify the Open Circuit Potential (OCP) and identify the propensity for pitting to occur. The CPP testing was performed according to ASTM G61, *Standard Test Method for Conducting Cyclic Potentiodynamic Polarization Measurements for Localized Corrosion Susceptibility of Iron-, Nickel-, or Cobalt-Based Alloys*. Prior to specimen

introduction, the test solution was heated to the desired temperature 50 °C (122 °F) or 77 °C (171 °F). Tests were conducted under quiescent (no gas purge), deaerated (constant pure nitrogen purge), and oxygenated (constant pure oxygen purge). For tests conducted with gas purging, the prepared test solution was purged with gas (nitrogen or oxygen) for one hour prior to specimen introduction and continued throughout the test. Fig. 2 shows the result of a CPP from AY-102 carbonate waste.

Nitrogen purging was used to maintain a deaerated condition such that the oxygen reduction reaction was minimized or eliminated. Thus, under deaerated conditions the cathodic reactions would be dominated by other reducible species in the solution (i.e., nitrite, nitrate) or through water reduction (if the potential was negative enough). To evaluate the effect of a moderately oxidizing condition, pure oxygen gas was purged in some cases. These tests were intended to partially mimic the conditions that might develop due to radiolysis of water to produce peroxide without the experimental complications associated with peroxide decomposition.

Prior to CPP testing, the OCP was monitored for 18 hours. Then the potential scan was started from -100 mV vs. OCP with a scan rate of 0.17mV/s. The scan was reversed at 1V vs. a saturated calomel electrode (SCE) or when the current reached 1mA/cm², whichever occurred first. In a few cases, a longer-term steady state value for the corrosion potential was desired. In these cases, the sample was prepared with the same method mentioned above and the OCP was measured continuously with a potentiostat for the desired amount of time.

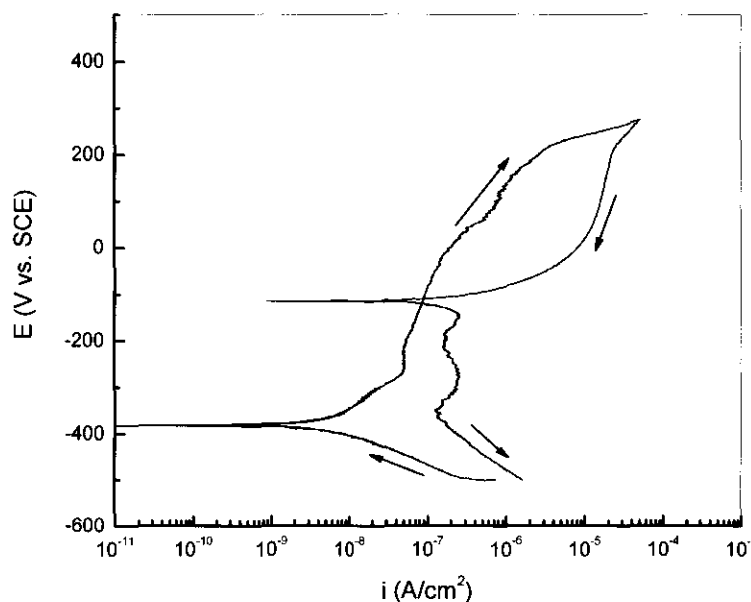


Fig. 2. Typical Cyclic Potentiodynamic Polarization Curve for Tank 241-AN-107 Standard Solution at pH 11 and 50 °C.

SLOW STRAIN RATE TESTING

The SSR testing is used to identify the propensity for SCC to occur in a specimen in a given chemical environment. The SSR testing was performed according to the guidelines provided in ASTM G129, *Standard Practice for Slow Strain Rate Testing to Evaluate the Susceptibility of Metallic Materials to Environmentally Assisted Cracking*, using cylindrical tensile specimens at a constant extension rate of

10⁻⁶ in/in-s. To perform the tests, the specimen was placed into a Teflon test cell and the load applied using pull rods that entered the cell through sliding seals.

After insertion of the specimen and pull rods into the load frame, the solution of interest was introduced and heated to either 50 °C (122 °F) or 77 °C (171 °F). Tests were either conducted at open circuit or at an applied potential against a reference electrode (vs. SCE) maintained at room temperature using a Luggin probe/salt bridge that was filled with the test solution. A platinum flag was used as a counter electrode.

Post-test analysis consisted of stereographic optical examination at 10 – 63x, metallographic cross-sectional analysis, and scanning electron microscopy (SEM). For AY-102, the fracture surface of each of the test samples was examined using the SEM to identify regions of intergranular fracture. In some cases there was a discrepancy between conclusions drawn based on stereo-microscope examinations and conclusions drawn based on SEM examination. That is, in some cases stereo-microscopy indicated no evidence of secondary cracking on the shafts of the samples, but intergranular fracture features were seen using the SEM, and in some cases stereo-microscopy indicated secondary cracking on the shafts of the samples, but no intergranular features were observed using the SEM. Table IV and Fig. 3 show selected results from the SSR testing for AN-107.

Table IV. Selected Slow Strain Rate Test Results for Tank 241-AN-107

Chemistry	pH	Applied Potential (mV vs. SCE)	Failure Time (hrs)	Failure Strain (%)	Maximum observed crack (µm)	Estimated Crack Growth Rate (mm/sec)	Degree of SCC
Air@100°C			55.5	27.1			
Standard	11	+100	73.7	24.9	326	1 x 10 ⁻⁶	Moderate
Standard	11	+100	70.5	24.7	186	7 x 10 ⁻⁷	Moderate
Standard	11	0	65.2	23.7	138	6 x 10 ⁻⁷	Moderate
Standard	11	0	80.4	27.5	425	2 x 10 ⁻⁶	Moderate
End point	10	-50	78.3	26.7	n/a	0	None
No nitrite	11	0	21.4	7.9	Not. Meas.	N/A	Major
No nitrite	11	0	25.0	8.6	Not. Meas.	N/A	Major
No nitrite	11	0	26.4	9.2	Not. Meas.	N/A	Major

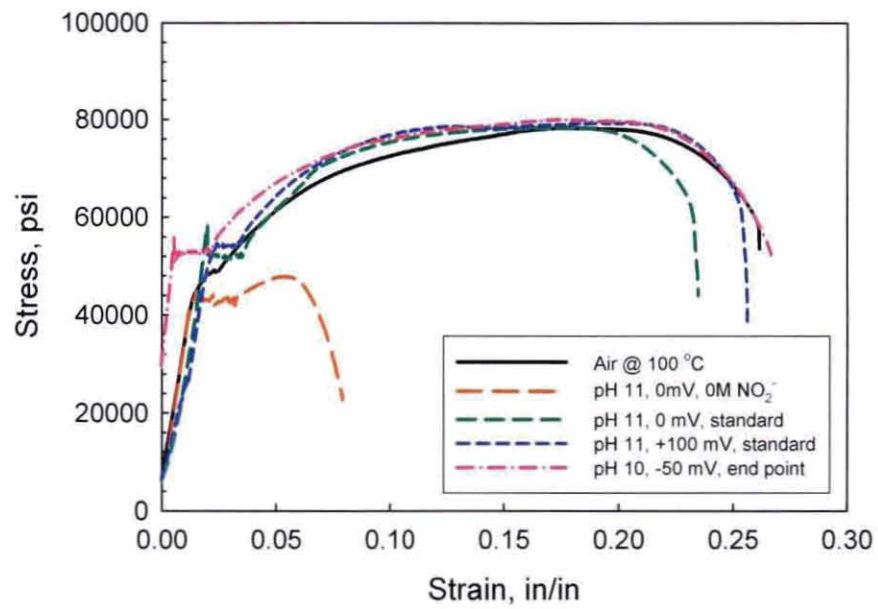


Fig. 3. Selected Results from Slow Strain Rate Testing for Tank 241-AN-107.

Where evidence of SCC was present, metallographic cross sectional analysis was utilized to estimate a crack growth rate by dividing the maximum crack length observed from SEM or cross-sectional analysis by the time to failure (total test time). The same approach was used to estimate SCC growth rates from SSR tests data. For the purposes of semi-quantitatively comparing the SSRT results, the estimated crack growth rate (CGR) was divided into four classifications as shown in Table V.

Table V. Crack Growth Estimates from Slow Strain Rate Testing

Degree of SCC	Estimated CGR (mm/s)	Estimated CGR (in/s)
Major	$\geq 3 \times 10^{-6}$	$\geq 1.2 \times 10^{-7}$
Moderate	$3 \times 10^{-6} - 5 \times 10^{-7}$	$1.2 \times 10^{-7} - 2 \times 10^{-9}$
Minor	$\leq 5 \times 10^{-7}$	$\leq 2 \times 10^{-9}$
None	No indications of SCC	

Note that the crack growth rates determined from the SSR tests should be used with caution and only for comparative purposes. Furthermore, the crack growth rates estimated from the SSR test results should not be compared with rates determined in constant load crack growth rate tests using compact tension specimens. The SSR tests crack growth rates tend to be higher because of the imposed continued straining of the specimens; a condition unrealistic for storage tanks.

The time-to-failure and the strain at failure of the specimens wasn't always consistent with the presence of SCC. Also, the degree of SCC was not easily established from these parameters. Therefore, the occurrence of SCC was always confirmed by both visual inspection and SEM examination, and the severity of SCC was determined from the estimated crack growth rate as described above.

K_{ISCC} AND CRACK GROWTH RATE TESTING USING COMPACT TENSION SPECIMENS

The measurement of K_{ISCC} is used to determine whether a crack initiated under the SSR testing would continue to grow and to determine the minimum flaw size that the Ultrasonic Testing (UT) has to detect when inspecting flaws for through wall penetration of a tank. The K_{ISCC} and crack growth rate (CGR) tests were performed using pre-cracked ½-T (0.5 inch wide) compact tension (CT) specimens.

Tests performed on AN-107 tank chemistries were done using a CT load. However, several of the tests showed very low crack growth rates, such that the estimated rates were at the lower limit of resolution of the measurement technique. As such, much of the data contained measurement noise that hindered a thorough analysis. Fig. 4 shows the ranges of crack growth rates found in the AN-107 testing for present and end-point chemistries along with SRS tests conducted with the Wedge Open Load (WOL) technique on solutions containing 5 M sodium nitrate (DP-MS-77-25, *Temperature Dependence of Nitrate Stress Corrosion Cracking*). The tests for AN-107 showed that the low measured crack growth rates for AN-107 would not have been detected by the WOL testing and would have been report as having no crack growth rate.

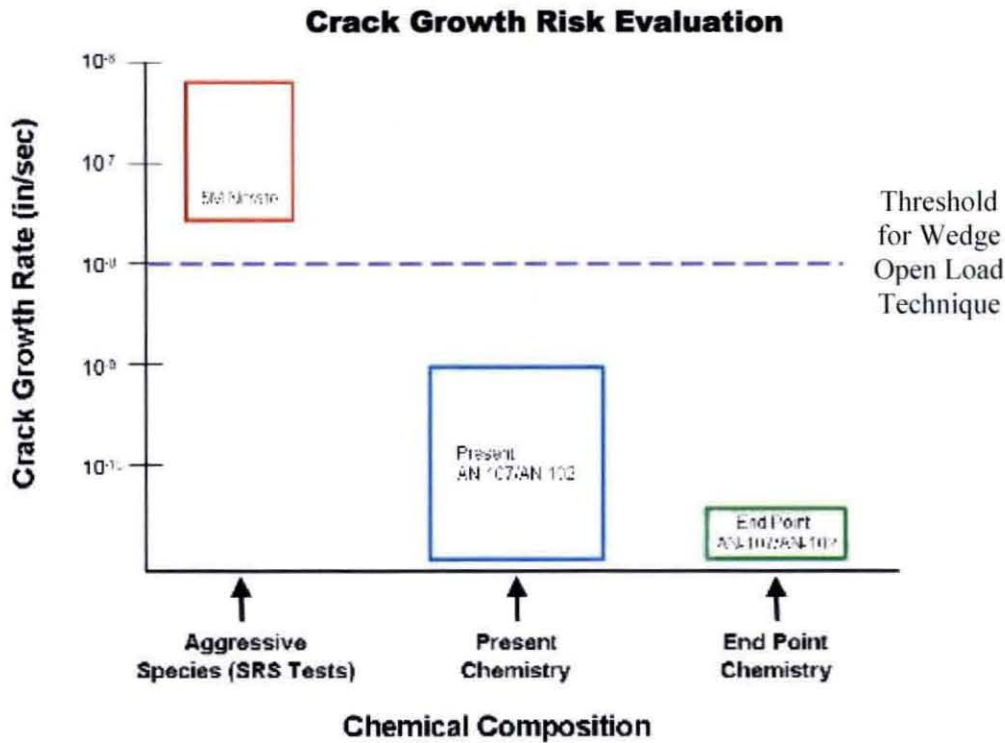


Fig. 4. Crack Growth Risk Evaluation.

To avoid the measurement noise encountered in the AN-107 tests at very low crack growth rates, the AY-102 tests were run at a constant displacement rate rather than a constant load. The technique is referred to as the "Dynamic-K" test. There were two advantages to this technique. The first is that both K_{ISCC} and CGR can be estimated from the same test data. Constant load test allows estimation of a CGR, but only if cracking occurs. In addition, constant load testing only allows for a determination as whether K_{ISCC} is over or under the K_I selected for a given test. This approach requires that several tests be conducted, using trial and error, to effectively "bracket" the K_{ISCC} value for the steel at a given set of test conditions. The second advantage of the dynamic-K test is that the tests can be run more quickly than the standard constant load test. Previous constant load tests were typically conducted for 30 days. Dynamic-K tests take approximately 7-21 days to complete, depending on the specific test requirements. The advantages are not realized, however, if the tests are stopped prior to extensive cracking.

The dynamic-K tests were performed on the same loading frames as were used for the slow strain rate tests. The Dynamic-K tests were conducted as slowly as could be achieved, which is in the order of 5×10^{-7} in/in-s, compared to a nominal rate of 10^{-6} in/in-s for SSR. The standard CT specimens had to be modified to be accommodated by the SSR loading frames. Some of the samples were fatigue pre-cracked to a greater depth than in previous tests, and all specimens were side-grooved.

All tests were conducted in Teflon cells heated to the test temperature of 50 °C (122 °F) or 77 °C (171 °F) prior to applying the desired load. Tests were conducted at either open circuit or at an applied potential. For the tests at the OCP, the potential was monitored with a high impedance voltmeter and a SCE reference electrode. The SCE reference electrode was maintained at room temperature and communicated with the rest of the test cell by means of a Luggin probe/salt bridge that was filled with the waste simulant. For the tests at applied potential, an additional platinum flag counter electrode was

included in the test cell and a potentiostat was used to control the potential to the desired value. All CGR experiments were performed under quiescent conditions.

The applied load and displacement for the test samples were monitored and recorded continuously during the tests. In addition, the direct current potential drop (DCPD) technique was used to monitor crack growth in situ. The DCPD technique involves applying a constant current of 20 amps across the two sides of the crack while the potential drop across the crack is recorded. Any crack propagation during the test will increase the resistance of the sample and this will be reflected by a change in potential.

To determine if crack propagation had taken place, both the crack length and displacement measurements were used. A significant DC potential drop increase, beyond the noise in the data, was considered indicative of crack growth. A reduction in the loading rate was also considered indicative of crack growth, as it indicates an increase in specimen compliance. The initial tests performed were continued well past failure of the sample. The majority of the tests were performed only until a predefined limit of K_I was reached (either nominal 25 or 35 ksi $\sqrt{\text{in}}$), or until the measurements indicated cracking, whichever was first. Crack morphology was always verified by microscopy.

Following testing, samples were sectioned longitudinally and one half of the sample was mounted and prepared for metallographic examination while the other half of the sample was cooled in liquid nitrogen, and then overloaded in the laboratory to reveal the fracture surface. Fracture surfaces were examined using the SEM for evidence of intergranular fracture features, indicative of high pH SCC, as described above for the SSR test specimens.

The morphologies of the fracture surfaces observed in the SEM indicated whether or not crack growth had occurred, and whether or not any crack growth that had occurred was as a result of SCC. Four types of fracture surface were expected during examination of the samples; fatigue, ductile, intergranular, and brittle overload. From the inspection of the fracture surfaces, the known test conditions, and the load and DCPD data, estimates of both K_{ISCC} and CGRs were possible. Fig. 5 shows the scanning electron microscope for CT-1, 1N carbonate – 1N bicarbonate solution.

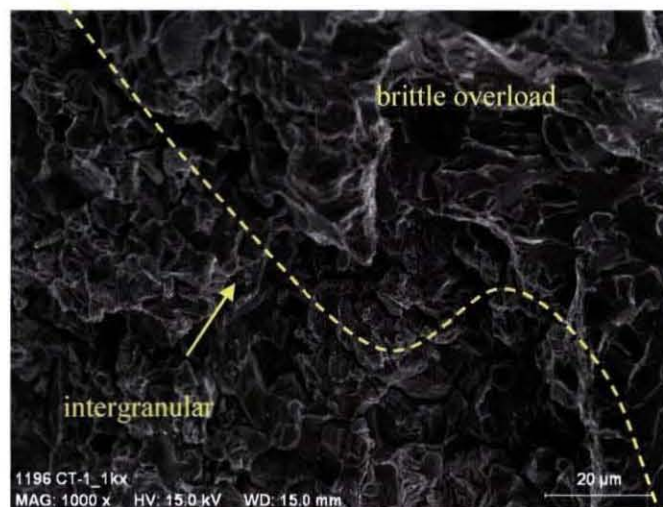


Fig. 5. An Electron Micrograph of the Intergranular SCC / Brittle Overload Interface from 241-AY-102 Performed in 1N Carbonate / 1N Bicarbonate Solution at 50°C and at Potential -615 mV vs. SCE, Loaded Well Past Crack Initiation.

SUMMARY OF CORROSION BEHAVIOR

Significant progress has been made toward implementing a new corrosion chemistry basis for the DSTs at Hanford. When completed the new basis will eliminate further sodium hydroxide additions that consume tank space and extend the RPP mission lifetime. Pitting corrosion and stress corrosion cracking work is complete on two waste types that envelop the DST waste at Hanford. The remaining testing is expected to be completed in 2008.

Pitting Corrosion

From the perspective of localized corrosion both AN-107 and AY-102 waste simulants have a low propensity for corrosion. The tank AN-107 waste simulants in general proved to be more aggressive than those for tank AY-102 waste simulants. This difference is primarily a result of chemistry differences. For example, the nitrate and chloride concentrations (aggressive species) in the AN-107 simulant were greater than in AY-102. The concentration ratio of possible inhibiting species (e.g., nitrite, carbonate, hydroxide, aluminate) to aggressive species in AN-107 was lower than that in AY-102.

The propensity of the tank steel to pitting corrosion in the AN-107 and AY-102 simulants is illustrated in Fig. 6 as a function of inhibiting species (i.e., nitrite and hydroxide) and aggressive species (i.e., nitrate and chloride). The points labeled Argentina data were from the work conducted by Carranza.

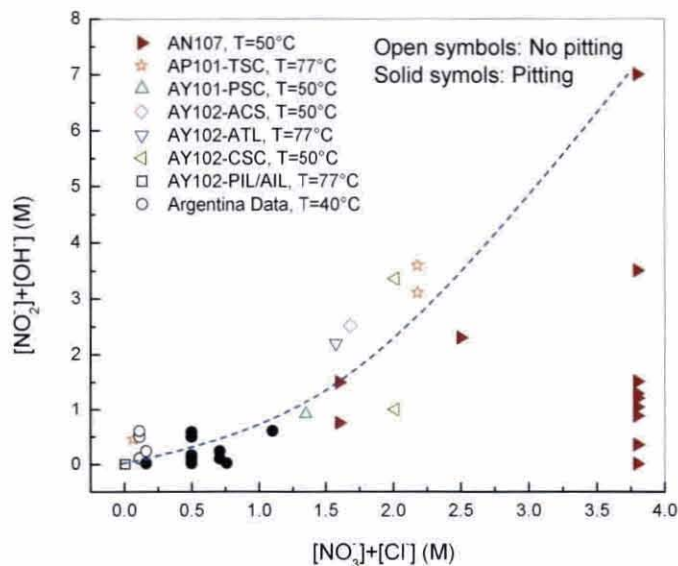


Fig. 6. The Propensity of Materials to Pitting Corrosion as a Function of Nitrite, Hydroxide Concentration and Nitrate, Chloride Concentration.

At each nitrate + chloride concentration level there appeared to be a critical nitrite + hydroxide concentration level above which the material was protected from localized corrosion. When the nitrate concentration was 3.7 M (as for AN-107), pitting corrosion was observed even when the nitrite concentration was 7 M. Although this indicates that a significantly higher nitrite concentration level is needed to completely inhibit pitting corrosion, the increase in the nitrite concentration from 0 M to 7 M in fact moved the pitting potential from below OCP to approximately 500 mV more positive than OCP

(-397 mV vs. SCE). Thus, even though pitting was not completely eliminated, this significantly increased the difference between OCP and pitting potential and thus reduced the likelihood of localized corrosion in the tanks.

Stress Corrosion Cracking

Nitrite concentration and the nitrite/nitrate concentration ratio were found to have a pronounced influence on SCC susceptibility in AN-107. Fig. 7 shows the effects of the nitrite/nitrate concentration ratio as a function of applied potential on SCC susceptibility. These data show that at any given potential, SCC can be mitigated by increasing the nitrite/nitrate ratio and at a constant nitrite/nitrate ratio the propensity for SCC decreases with decreasing OCP.

The exact mechanism of inhibition by which nitrite ions so effectively reduce the propensity for SCC is not understood. Similarly, carbonate and aluminate species appear to provide some inhibition to localized corrosion and SCC though, again, the mechanism is unclear. Ranges of nitrite ion concentration and electrochemical potential have been identified that significantly reduces any propensity for SCC. Work is in progress to define similar areas for carbonate and aluminate.

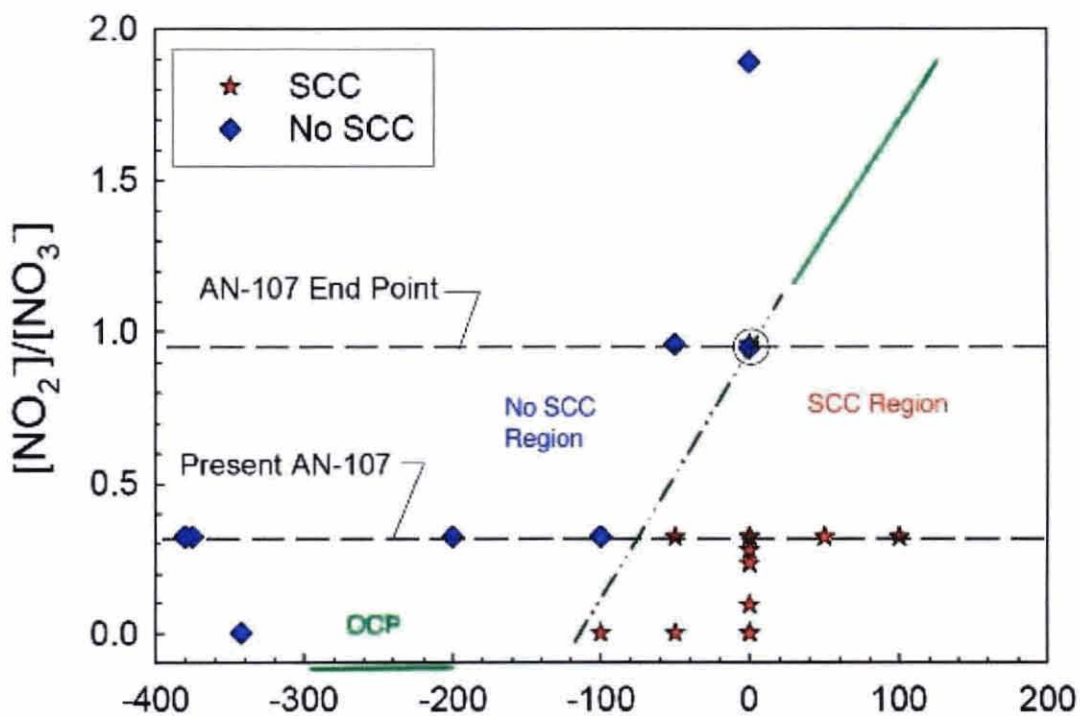


Fig. 7. Stress Corrosion Cracking Region in Tank 241-AN-107 Waste Simulants.

REFERENCES

“Standard Test Method for Conducting Cyclic Potentiodynamic Polarization Measurements for Localized Corrosion Susceptibility of Iron-, Nickel-, or Cobalt-Based Alloys”, ASTM G61

WM2008 Conference, February 24 - 28, 2008, Phoenix, AZ

“Standard Practice for Slow Strain Rate Testing to Evaluate the Susceptibility of Metallic Materials to Environmentally Assisted Cracking”, ASTM International (2005).

Johnson, H. H. “Calibrating the Electric Potential Method for Studying Slow Crack Growth”, Materials Research and Standards, Vol 5, No 9, September 1965, pp 442-445.

R.M. Carranza, C.M. Giordano, E. Sáenz, and D.R. Weier, Paper 06635, Corrosion 06, NACE International, Houston (2006)

J.A. Donovan, Temperature Dependence of Nitrate Stress Corrosion Cracking, E. I. DuPont Nemours and Co., DP-MS-77-25, October 1977